Human keratin hydrogels support fibroblast attachment and proliferation in vitro

Article *in* Cell and Tissue Research · January 2012

DOI: 10.1007/s00441-011-1295-2 · Source: PubMed

4 authors, including:

Francesca Taraballi
Houston Methodist Research Institute
150 PUBLICATIONS **3,143** CITATIONS

SEE PROFILE

Lay Poh Tan
Nanyang Technological University
145 PUBLICATIONS **5,211** CITATIONS

SEE PROFILE

Cell Tissue Res (2012) 347:795–802
DOI 10.1007/s00441-011-1295-2

REVIEW

Human keratin hydrogels support fibroblast attachment and proliferation in vitro

Shuai Wang · Francesca Taraballi · Lay Poh Tan · Kee Woei Ng

Received: 15 October 2011 / Accepted: 21 November 2011 / Published online: 28 January 2012

Abstract Human hair keratins have a strong potential for development as clinically relevant biomaterials because they are abundant and bioactive and are a realistic source of autologous proteins. Specifically, keratins have the propensity to polymerize in an aqueous environment to form hydrogels. In order to evaluate the suitability of keratin hydrogels as substrates for cell culture, we have fabricated hydrogels using keratins extracted from human hair by inducing polymerization with Ca^{2+}; these hydrogels exhibit highly branched and porous micro-architectures. L929 murine fibroblasts have been used in a preliminary cell culture study to compare the in vitro biocompatibility of the keratin hydrogels with collagen type 1 hydrogels of similar viscoelastic properties. Our results reveal that keratin hydrogels are comparable with collagen hydrogels in terms of the promotion of cell adhesion, proliferation and the preservation of cell viability. Interestingly, cells remain clustered in proliferative colonies within the keratin hydrogels but are homogeneously distributed as single cells in collagen hydrogels. Collectively, our results demonstrate that keratin hydrogels can be used as substrates for cell culture. Such gels might find applications as templates for soft tissue regeneration.

This research was supported by the National Medical Research Council—New Investigator Grant (NMRC/NIG/1005/2009).

S. Wang · F. Taraballi · L. P. Tan · K. W. Ng (✉)
School of Materials Science and Engineering,
Nanyang Technological University,
50 Nanyang Avenue,
Singapore 639798, Singapore
e-mail: kwng@ntu.edu.sg

S. Wang
e-mail: WANGSHUAI@NTU.EDU.SG

F. Taraballi
e-mail: FTARABALLI@NTU.EDU.SG

L. P. Tan
e-mail: LPTAN@NTU.EDU.SG

Keywords Keratin · Hydrogel · Scaffold · Cell culture · Tissue engineering

Introduction

In order to emulate the in vivo scenario more accurately, scientists have devoted much attention to the creation of three-dimensional (3D) models in vitro to study cellular behaviour or to engineer transplantable tissues (Abbott 2003; Kale et al. 2000). Among these, the use of hydrogels is one of the most established because of their close resemblance to the in vivo histo-architecture of the natural extracellular matrix (ECM; Geckil et al. 2010; Mather and Tomlins 2010). Hydrogels are crosslinked 3D networks of either natural or synthetic polymers. Those hydrogels based on synthetic polymers have more controllable physical properties and are more reproducible. However, problems have been experienced with these polymers, such as poor biocompatibility, lack of bioactivity and little resemblance to the natural environment (Dawson et al. 2008; DeLong et al. 2005; Schmedlen et al. 2002; Thonhoff et al. 2008).

The feasibility of using natural materials including polysaccharides and proteins in the form of hydrogels has been well-demonstrated. Among these materials, ECM proteins such as collagen, elastin, fibrin and hyaluronic acid exhibit prominent bioactivity in biomedical applications (Kim et al. 2007; Lee et al. 2001). Collagens are particularly popular in various forms for diverse applications (Auger et al. 1998; Meena et al. 1999; Nerem 2000). However, these collagens are mostly of animal origin, with the associated risks of provoking human immune response and pathogen transfers thus restricting their clinical applications (Lynn et al. 2004; Song et al. 2006). To address this problem, human collagen derived from donor cadavers, placentas, adipose tissue and

aborted fetuses are used (Choi et al. 2010). Alternatively, recombinant human collagen has been employed to minimize the immune response (Yang et al. 2004). The use of human fibrin as a hydrogel in the clinic is also well documented (Currie et al. 2001). Although these human proteins have worked well, limited sources and high costs hamper their widespread use clinically. Therefore, the demand for an alternative protein that is of human origin and that can be processed into a hydrogel for various clinical applications is anticipated.

In comparison with other materials, human hair keratins possess distinct advantages such as being abundant and bioactive, having a strong ability to self-assemble into hydrogels and being a realistic source of autologous proteins. Soluble human hair keratins can be extracted easily from human hair by using cocktails of reducing agents in alkaline or acidic environments (Fujii et al. 2008; Wrzesniewska-Tosik and Adamiec 2007). These keratin solutions are capable of polymerizing to form hydrogels that have been used successfully in vivo as a physical barrier to prevent the infiltration of inflammatory cells following cell transplantation (Nakaji-Hirabayashi et al. 2008) and also as an internal haemostat (Aboushwareb et al. 2009; Hill et al. 2010). Although keratins belong to the family of intermediate filaments that are intracellular cytoskeleton proteins (Szeverenyi et al. 2008), they contain the cell adhesion motif LDV (leu-asp-val), which is recognized by $\alpha_4\beta_1$ integrin (Makarem and Humphries 1991), suggesting that keratins can function as an extracellular substrate for cell attachment and subsequently can support cell growth and development (Verma et al. 2008). Indeed, Sierpinski et al. (2008) have shown that keratin hydrogels can enhance nerve regeneration in vivo. Keratins in the form of coatings, fibres and films have also shown promising cytocompatibility (Reichl 2009; Rouse and Van Dyke 2010). Here, we report the fabrication and characterization of a human keratin hydrogel and demonstrate its potential as a soft tissue regeneration template.

Materials and methods

Materials

Sodium sulphide (Na_2S), calcium chloride ($CaCl_2$), paraformaldehyde (PFA), bovine serum albumin and dialysis tubings (molecular weight cut-off=12,400 Da) were purchased from Sigma Aldrich. Dulbecco's modified Eagle's medium (DMEM), fetal bovine serum (FBS), non-essential amino acids, L-glutamine, sodium pyruvate, penicillin-streptomycin and 0.25% trypsin were purchased from Gibco (Invitrogen). The PicoGreen DNA quantification kit, calcein AM and secondary goat anti-mouse horseradish-peroxidase-conjugated (HRP) antibody were purchased from Molecular Probes (Invitrogen). SimplyBlue SafeStain solution, precast 4%-12% Bis-TRIS gels, lithium dodecyl sulphate sample buffer, sample reducing agent, MOPS SDS running buffer, NuPAGE antioxidant and iBlot gel transfer stacks were purchased from Invitrogen. Primary mouse polyclonal antibody against total human hair keratins (clone AE13) was obtained from Abcam. Rat tail collagen type 1 was purchased from BD biosciences. The 660-nm protein quantification kit and Super Signal West Pico chemiluminescent substrate were purchased from Pierce.

Extraction and purification of human hair keratins

Human hair was obtained from three local hair salons, with no distinction being made with regard to age, gender or ethnic group. Random hair samples were first washed with soap, followed by 70% ethanol, rinsed extensively with water and air-dried. The cleaned hair was delipidized by being soaked in a mixture of chloroform and methanol (2:1 v/v) for 24 h. The delipidized hair was subsequently air-dried and cut into 1-cm-long fragments for keratin extraction. Delipidized hair fragments (50 g) were immersed in 1 l 0.125 M Na_2S solution and incubated at 40°C for 4 h. The resulting mixture was filtered and exhaustively dialyzed against 2 l deionized water, by using cellulose tubing. The dialysis step was repeated six times. Keratin concentration was thereafter quantified by using the 660-nm protein assay kit.

Coomassie blue staining and Western blotting

Keratin (10 μg for coomassie blue staining or 1 μg for Western blot) in solution was mixed with 5 μl LDS sample buffer and 2 μl sample reducing agent and made up to 20 μl with deionized water. The samples were heated at 75°C for 10 min prior to gel electrophoresis in NuPAGE Novex 4-12% Bis-TRIS gels, at 120 V for 90 min. Gels were subsequently washed three times with deionized water and were either stained for 60 min with Coomassie blue (SimplyBlue SafeStain solution) or transferred onto nitrocellulose membranes by using the iBlot Dry Blotting System at 20 V for 6 min. Membranes were blocked with 5% dry milk in phosphate-buffered saline (PBS) containing 0.05% Tween-20 (PBST) for 30 min and then incubated with a mouse polyclonal primary antibody against total human hair keratins (1:1000 in blocking solution) for 60 min at room temperature. Thereafter, the membranes were washed with PBST and incubated with HRP-conjugated goat anti-mouse secondary antibody (1:4000 in blocking solution) for 30 min at room temperature. Chemiluminescence was generated by adding the Super Signal West Pico chemiluminescent substrate.

Fourier-transformed infrared spectroscopy

Fourier-transformed infrared (FTIR) spectroscopy was carried out in attenuated total reflection (ATR) mode by using a single reflection diamond element. Aliquots of 5 μl of each keratin solution, before and after dialysis, were deposited on the ATR plate and spectra were recorded after solvent evaporation at a resolution of 2 cm^{-1}. The ATR-FTIR spectra were reported after normalization on the Amide I band area to compensate for possible differences in the sample sizes and after binomial smoothing (11 points) of the spectra.

Fabrication of keratin hydrogel

The keratin solution was adjusted to a concentration of 10 mg/ml and sterile-filtered with a 0.2-μm cellulose filter. Keratin gelation was started by mixing the required volume of keratin solution with 1 M $CaCl_2$ solution at a ratio of 50:1 (v/v). The mixture was kept in an incubator at 37°C and 5% CO_2 overnight for complete gelation. The resulting keratin hydrogel was washed four times with excess sterile deionized water prior to use.

Fabrication of collagen hydrogel

Collagen hydrogels (1 mg/ml) were prepared according to the manufacturer's instruction. Briefly, the required volume of collagen was neutralized with 1 M NaOH in PBS and allowed to gel at 37°C for 30 mins.

Oscillatory rheology

Oscillatory rheology experiments were performed at 37°C on a rheometer (Anton Paar, Germany) with a 50-mm diameter stainless steel parallel plate. Keratin or collagen hydrogel was formed from an initial volume of 6 ml solution (10 mg/ml and 1 mg/ml, respectively) in a 50-mm Petri dish. After zeroing the gap height, the parallel plate was lowered until it touched the hydrogel surface. In both hydrogel samples, the same gap height of 3.1 mm was recorded at this instance. For frequency sweep, the storage modulus (G') was monitored as a function of angular frequency.

Scanning electron microscopy

The micro-architecture of keratin and collagen hydrogels was examined by scanning electron microscopy. Keratin and collagen hydrogels were frozen at −20 ° C for 8 h and subsequently lyophilized for 2 days. The resulting sponges were gold-sputtered at 18 mA for 10 s and observed under a scanning electron microscope (JSM-6360, JEOL, USA) at an accelerating voltage of 5 kV.

Culture of L929 fibroblasts on keratin and collagen hydrogels

Keratin and collagen hydrogels were produced in 24-well culture plates as described above, by using the same starting volume of 1 ml. They were equilibrated with DMEM supplemented with 10% FBS at 1 day before cell seeding. L929 murine fibroblasts were maintained on tissue culture polystyrene (TCPS) in DMEM supplemented with 10% FBS, 2 mM L-glutamine, 1 mM sodium pyruvate, 0.1nM non-essential amino acids, 100 U/ml penicillin and 100 μg/ml streptomycin. Cells were harvested from a sub-confluent culture by using 0.25% trypsin, counted by means of a haemocytometer and seeded on top of the keratin and collagen hydrogels at a density of 10,000 cells/cm^2.

Histological examination

Cell-populated hydrogels cultured for 6 days were fixed in 4% PFA for 48 h at room temperature and embedded in paraffin by using standard protocols. Serial sections (5 μm thick) were cut, mounted on glass slides and stained with haematoxylin and eosin (H&E). Brightfield images were obtained by using an upright phase contrast light microscope (CKX41, Olympus, Japan).

Results and discussion

Characterization of keratin extracts

Coomassie blue staining showed that the human hair extracts consisted in basic keratin monomers (~50 kDa), acidic keratin monomers (~45 kDa) and keratin heterodimers (Fig. 1a). Two bands in the acidic keratin region indicated the occurrence of at least two acidic keratin subtypes (Langbein et al. 1999, 2001). Multiple bands within the keratin dimer region indicated different heterodimer combinations. The identity of human hair keratins was confirmed by blotting against total human hair keratins (Fig. 1b).

FTIR spectra of extracted keratin solution before and after dialysis displayed amide I (1700–1600 cm^{-1}) and amide II (close to 1500 cm^{-1}) peaks (Fig. 2), resulting from peptide bond vibrations typical of protein samples. In the spectra of samples before dialysis, the strong peaks at around 1100 cm^{-1} and 980 cm^{-1} could be assigned to SO_4^{2-} and $S_2O_3^{2-}$ groups, which were probably produced by the following secondary reactions during the extraction process:

$$2Na_2S + 2O_2 + H_2O \rightarrow Na_2S_2O_3 + 2NaOH$$

$$Na_2S_2O_3 + 2NaOH + 2O_2 \rightarrow 2Na_2SO_4 + H_2O$$

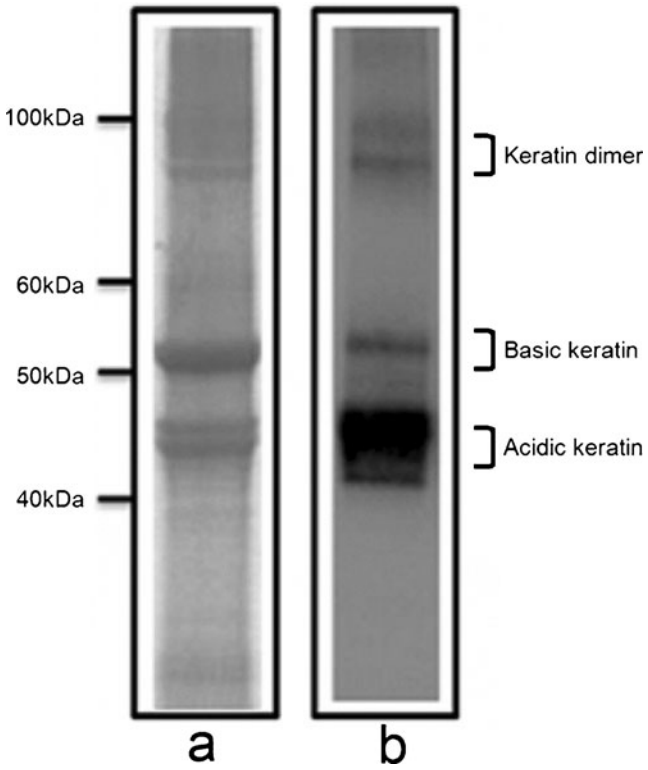

Fig. 1 Coomassie blue staining (**a**) and Western blot analysis (**b**) of soluble extracts from human hair indicate the presence of human keratin monomers and heterodimers

The $S_2O_3^{2-}$ group has two characteristic peaks at about 995 cm^{-1} and 1115 cm^{-1}, whereas the SO_4^{2-} group has only one characteristic peak at about 1100 cm^{-1} (Bandekar et al. 1995). The peak at around 1100 cm^{-1} might therefore be a result of overlapping peaks of both the SO_4^{2-} and $S_2O_3^{2-}$ groups. More importantly, these two peaks disappear after dialysis (Fig. 2), indicating the efficient removal of these contaminants.

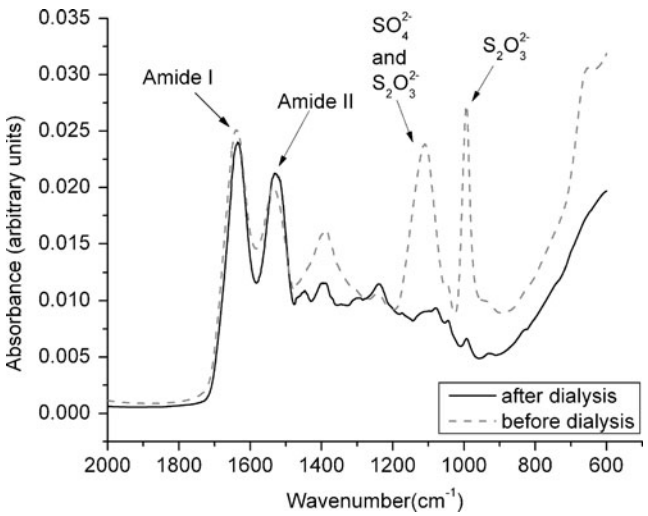

Fig. 2 FTIR spectra of human hair extracts show retention of proteins and removal of contaminants after dialysis

Physical properties of keratin and collagen hydrogels

Figure 3 shows the frequency dependence of the storage loss modulus for keratin and collagen hydrogels at 37°C. A typical shear thinning behaviour was evident: up to the frequency of 10 Hz, the storage modulus (G') was nearly constant (~5 Pa) followed by a rapid decrease beyond 10 Hz. For comparison, the rheological behaviour of collagen hydrogels was also measured and these showed shear thinning behaviour and a shear modulus similar to those of the keratin hydrogels. Therefore, keratin hydrogels have similar initial stiffness and viscoelastic properties as 1 mg/ml collagen, within our experimental conditions.

Representative scanning electron microscopic images of lyophilized keratin and collagen hydrogels are shown in Fig. 4. Both hydrogels exhibited highly porous and interconnected porous micro-architectures. Keratin hydrogels consisted in smaller pores with pore walls being made up of irregularly shaped and thin leaflets, which were highly branched (Fig. 4a). In contrast, collagen hydrogels had branching networks of long fibrous bundles, giving rise to larger pore structures (Fig. 4b).

Behaviour of L929 murine fibroblasts in keratin and collagen hydrogels

Cell proliferation was tracked by measuring the total amount of double-stranded DNA (dsDNA) in the cultures by using

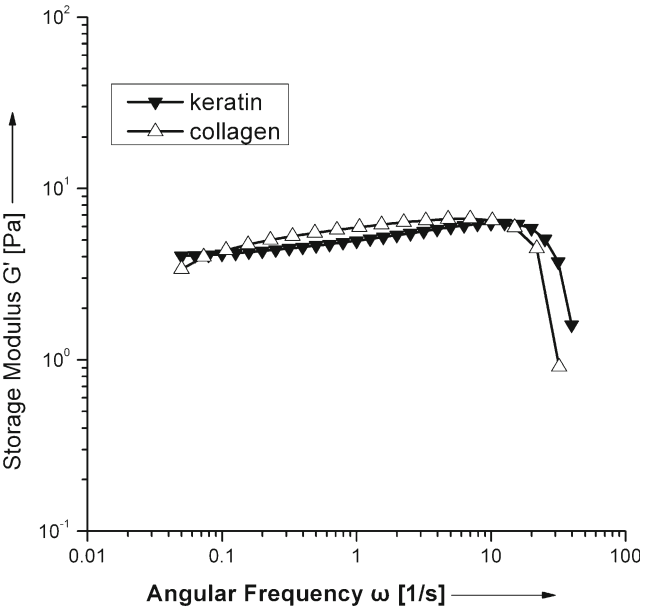

Fig. 3 Plot of storage modulus, G', as a function of frequency, at 37°C for keratin (▼) and collagen (Δ) hydrogels, suggesting similar viscoelastic properties of the two materials

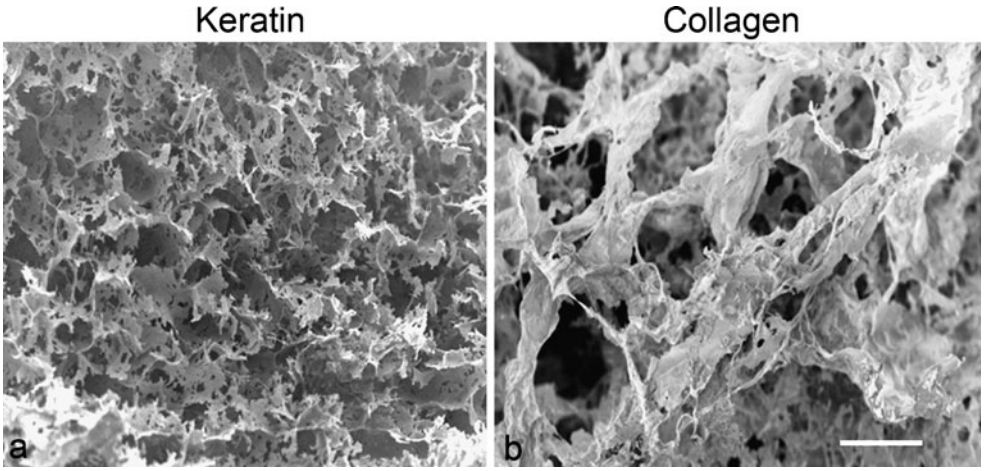

Fig. 4 Scanning electron microscopic images of lyophilized keratin (**a**) and collagen type 1 (**b**) hydrogels, showing their highly porous and interconnected microarchitecture. Pore sizes are smaller in the keratin hydrogel and pore walls comprise highly branched leaflets compared with the fibrous bundles in collagen hydrogels. *Bar* 200 μm

the PicoGreen assay (Fig. 5). On day 1 after cell seeding, almost equal amounts of dsDNA were recorded in all samples, suggesting that cell adhesion efficiency was comparable in all groups. Beyond day 2, cell proliferation on the keratin hydrogels began to lag behind that on the collagen hydrogels and controls, whereas proliferation in the controls was consistently higher than in both the hydrogel groups. Between day 2 to day 4 of culture, dsDNA levels in keratin hydrogels increased by four times, whereas that in the collagen and control groups increased by seven and ten times, respectively. Cell proliferation in all groups reached a plateau after day 10, possibly a result of contact inhibition and confluence-induced apoptosis. Collectively, despite the lower proliferation rate, dsDNA levels in the keratin hydrogels averaged 76% of that in the collagen hydrogels throughout the culture period.

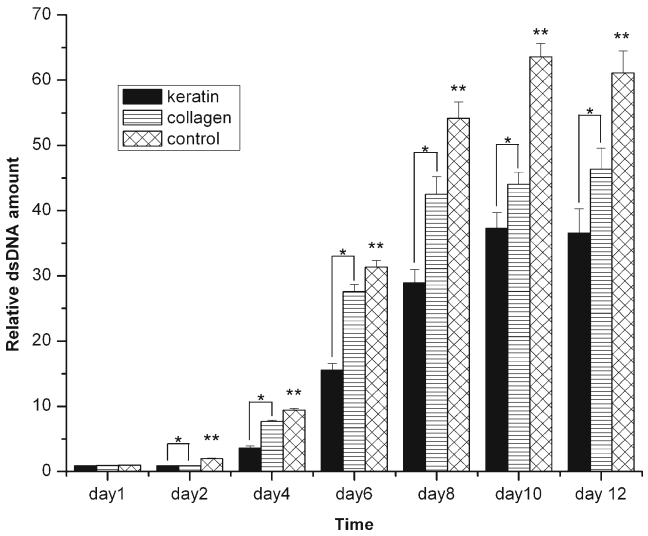

Fig. 5 Relative proliferation of L929 fibroblasts on keratin and collagen hydrogels in comparison with tissue culture polystyrene (*control*). Data represent relative double-stranded DNA (*dsDNA*) levels over 12 days of culture, normalized to controls at day 1, presented as means ± standard deviation of quadruplicate samples. *$P<0.05$ (Student's *t*-test), **$P<0.05$ (analysis of variance, control versus both hydrogel groups)

As the keratin hydrogels were opaque, the cell viability and morphology were visualized by fluorescent calcein AM staining, which labelled the cytoplasm of live cells in green. Cells in the control group, which were cultured on 2D surfaces in 24-well plates, developed the spindle shape typical of fibroblasts from day 2 of culture (Fig. 6a) and maintained their morphology over days 4 and 6 of culture (Fig. 6d, g). In comparison, cells on keratin hydrogels remained round until day 4 of culture (Fig. 6b, e), with spindle morphology appearing at day 6 of culture (Fig. 6h). Collagen hydrogels are among the most well-studied and established hydrogels for biomedical applications (Hunt and Grover 2010). We therefore used collagen type 1 hydrogels of similar mechanical properties for comparison. Cells on the collagen hydrogels remained round on day 2 of culture (Fig. 6c). A small proportion of the cells exhibited typical spindle morphology on day 4 of culture (Fig. 6f) and, by day 6 of culture, most cells were spindle-shaped (Fig. 6i). Apart from the differences shown in morphology, cells in both the control and collagen groups were distributed evenly across the culture surfaces over the entire culture period, achieving near 100% confluence by day 6 of culture (Fig. 6g, i). In comparison, cells also proliferated over the same culture period in the keratin group but they did so in localized clusters that were randomly distributed over the hydrogel (Fig. 6e, h).

Over the culture period of 6 days, the cell-seeded area on the keratin hydrogel surfaces contracted significantly (Fig. 7). The areas on the hydrogel surfaces on which cells were seeded contracted, whereas the rest of the surface area remained stable, resulting in the formation of a ring on the hydrogel surfaces. On day 4 of culture, the contracted areas made up about 65% of the original hydrogel surface area. This reduced to about 45% on day 6 of culture. This contraction was brought about by the differentiation of fibroblasts

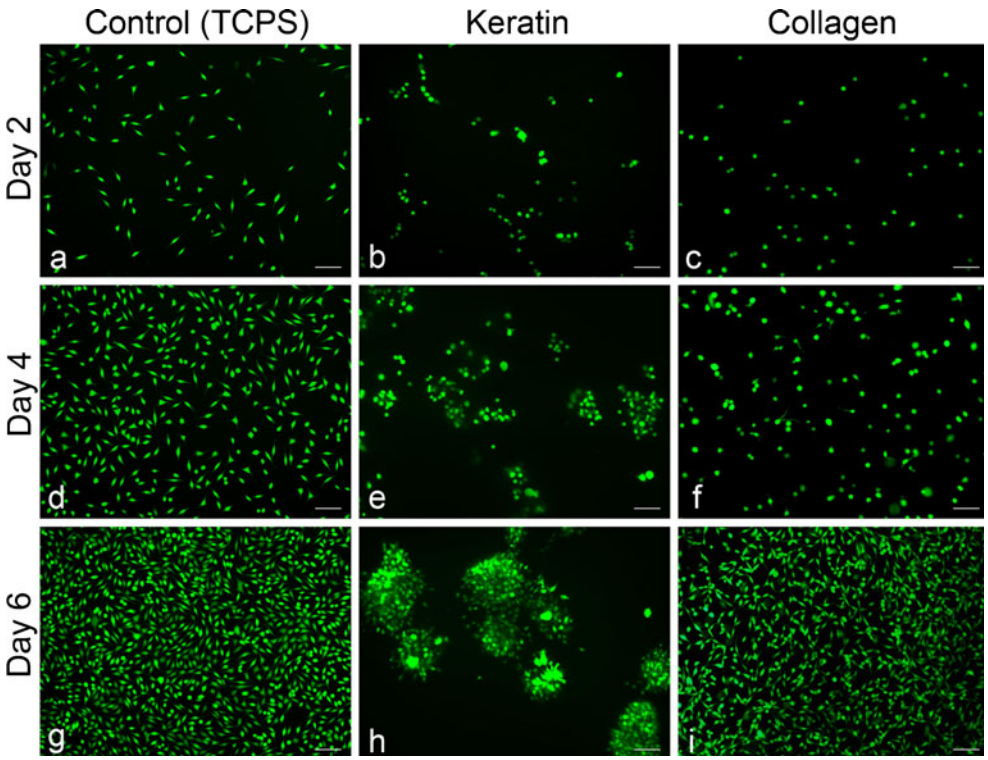

Fig. 6 L929 fibroblasts morphology and distribution. For all groups, cells were seeded at a density of 10,000/cm^2. Live cells were labelled green by calcein AM and observed under a fluorescent microscope at days 2, 4 and 6 post-seeding. **a**, **d**, **g** Cells grown on tissue culture plastic surfaces (*Control (TCPS)*) in 24-well plates showed typical spindle morphology at all time points and proliferated progressively to reach near 100% confluency by day 6. **b**, **e**, **h** Cells grown on keratin hydrogels exhibited spindle morphology by day 6 of culture and proliferated in localized clusters. **c**, **f**, **i** A small proportion of cells grown on collagen hydrogels exhibited spindle morphology at day 4 of culture. Cell distribution was comparable with that of controls. *Bars* 100 μm

into myofibroblasts, which express smooth muscle actin. This phenomenon has also been observed in other in vitro systems (Ng et al. 2004; Spector 2002) and in contracting wounds (Majno et al. 1971).

To assess cell penetration into the keratin and collagen hydrogels, cell-seeded samples were sectioned and processed for routine histological analysis with H&E staining. On day 2 of culture in the keratin group (Fig. 8a), cells were sparsely scattered on the hydrogel surfaces. On day 4 (Fig. 8c), a continuous monolayer of cells was evident on the hydrogel surface. A small proportion of cells penetrated downwards into the hydrogel, by about 500 μm in depth. At the same time, the keratin matrix became denser, especially in regions in which cells were distributed. On day 6 (Fig. 8e), significant cell penetration into the hydrogel was observed, up to a depth of 1 mm. The density of the keratin matrix continued to increase, suggesting further remodelling by the cells. Cells in the collagen hydrogels (Fig. 8b, d, f) showed similar penetration depths in comparison with the keratin hydrogels. However, in contrast with the keratin matrix, which appeared more globular, the collagen matrix was fibrous and less dense. Consistent with the fluorescent microscopy analysis in Fig. 6, more cells within the collagen hydrogels developed the fibroblast spindle morphology than those in keratin hydrogels.

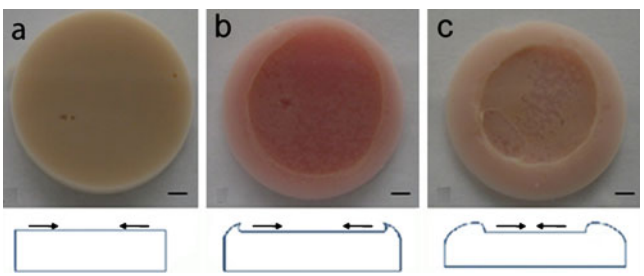

Fig. 7 Cell-induced keratin hydrogel surface contractions. Photographs of keratin hydrogel surfaces and corresponding cross-sectional representations before cell seeding (**a**) and 4 days (**b**) and 6 days (**c**) after cell seeding. Progressive contraction of cell-seeded surfaces was evident (arrows direction of contracting forces). *Bars* 2 mm

Despite similar stiffness being recorded in both the keratin and collagen hydrogels, the two environments clearly induced differences in cell behaviour. In addition to differing biochemical cues, such differences in cell morphology and growth profile might be influenced by microscale physical parameters such as pore size, fibre architecture and local material deformability (Pathak and Kumar 2011). In our case, the keratin hydrogels exhibited a micro-environment made up of smaller pores and finer branching networks compared with the collagen hydrogel (Fig. 4), suggesting a more restricted space and possibly a higher degree of local matrix deformation that could have limited cell proliferation, spreading and dispersal. However, the fibroblasts seemed to be able to remodel the keratin matrix in a manner similar to the remodelling of granulation tissue in a wound (Majno et al. 1971), as suggested by the increasing density of the keratin matrix over culture time (Fig. 8). Future studies will be conducted to study

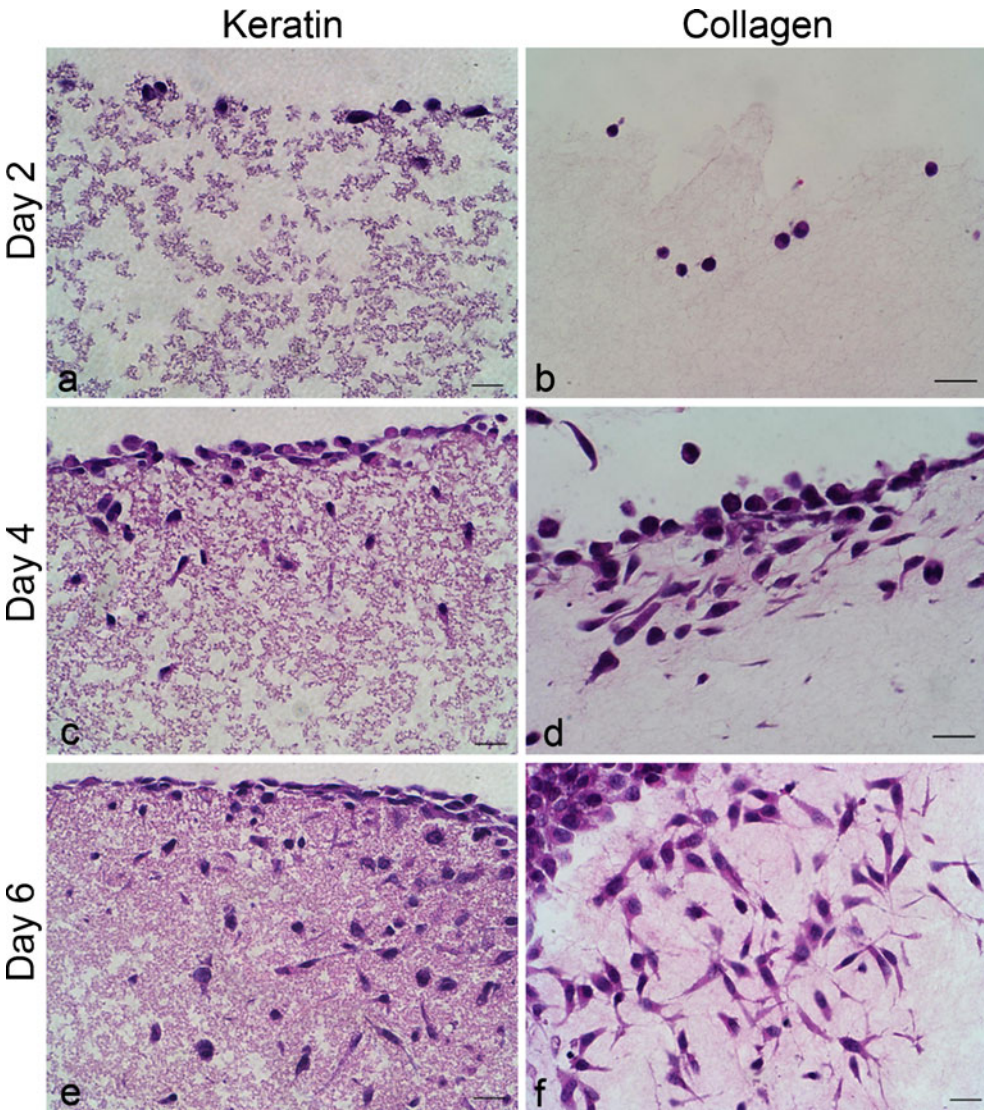

Fig. 8 Haematoxylin and eosin staining of cross-sectional samples of cell-seeded keratin (**a**, **c**, **e**) and collagen (**b**, **d**, **f**) hydrogels over days 2 (**a**, **b**), 4 (**c**, **d**) and 6 (**e**, **f**) of culture. Cell penetration into both hydrogels increased over time to reach about 1 mm depth from the top surface by day 6. The density of the keratin matrix appeared to increase with time in areas in which cells were distributed. *Bar* 100 μm

keratin matrix remodelling and to evaluate the influence of varying the keratin matrix micro-architecture, through variations in keratin concentration and polymerization parameters, on cell behaviour.

Concluding remarks

In this study, we have demonstrated the feasibility of extracting keratins from human hair, in agreement with the existing literature. Keratin quality has been preserved and the effective removal of any non-physiological chemicals from the keratin-solvent mixture has been achieved. The resulting keratin solution can be induced to form soft hydrogels in the presence of calcium ions. The storage modulus of these keratin hydrogels has been found to be about 5 Pa, similar to that of 1 mg/ml collagen type 1 hydrogels. The keratin hydrogels are highly porous but have pore sizes that are smaller than those in collagen hydrogels. Cell culture studies of L929 mouse fibroblasts have demonstrated that the keratin hydrogels support high cell viability over a 12-day culture period. Cell proliferation in the keratin hydrogels is less extensive than that in collagen type 1 hydrogels, with the cell population in the keratin hydrogels averaging 76% of that in the collagen hydrogels during the culture period. In addition, keratin hydrogels give rise to localized proliferative colonies compared with the homogeneously dispersed single cells within the collagen hydrogels. Nonetheless, fibroblasts are capable of penetrating and remodelling the keratin matrices, while remaining viable throughout the culture period studied. Given that keratins extracted from human hair have the advantages of being abundant and bioactive and are a realistic source of autologous material, we believe that keratin hydrogels have the potential to be further developed as a cell culture substrate and that they might find interesting applications in various biomedical applications such as templates for soft tissue regeneration.

Acknowledgement The authors are grateful to the Histopathology Unit (Biopolis Shared Facilities, A*STAR, Singapore) for their assistance in the histology work.

References

Abbott A (2003) Cell culture: biology's new dimension. Nature 424:870–872

Aboushwareb T, Eberli D, Ward C, Broda C, Holcomb J, Atala A, Van Dyke M (2009) A keratin biomaterial gel hemostat derived from human hair: evaluation in a rabbit model of lethal liver injury. J Biomed Mater Res B Appl Biomater 90B:45–54

Auger FA, Rouabhia M, Goulet F, Berthod F, Moulin V, Germain L (1998) Tissue-engineered human skin substitutes developed from collagen-populated hydrated gels: clinical and fundamental applications. Med Biol Eng Comput 36:801–812

Bandekar J, Sethna R, Kirschner M (1995) Quantitative determination of sulfur oxide species in white liquor by FT-IR. Appl Spectrosc 49:1577–1582

Choi JS, Yang HJ, Kim BS, Kim JD, Lee SH, Lee EK, Park K, Cho YW, Lee HY (2010) Fabrication of porous extracellular matrix scaffolds from human adipose tissue. Tissue Eng Part C Methods 16:387–396

Currie LJ, Sharpe JR, Martin R (2001) The use of fibrin glue in skin grafts and tissue-engineered skin replacements: a review. Plast Reconstr Surg 108:1713–1726

Dawson E, Mapili G, Erickson K, Taqvi S, Roy K (2008) Biomaterials for stem cell differentiation. Adv Drug Deliv Rev 60:215–228

DeLong SA, Moon JJ, West JL (2005) Covalently immobilized gradients of bFGF on hydrogel scaffolds for directed cell migration. Biomaterials 26:3227–3234

Fujii T, Murai S, Ohkawa K, Hirai T (2008) Effects of human hair and nail proteins and their films on rat mast cells. J Mater Sci Mater Med 19:2335–2342

Geckil H, Xu F, Zhang X, Moon S, Demirci U (2010) Engineering hydrogels as extracellular matrix mimics. Nanomedicine 5:469–484

Hill P, Brantley H, Van Dyke M (2010) Some properties of keratin biomaterials: kerateines. Biomaterials 31:585–593

Hunt NC, Grover LM (2010) Cell encapsulation using biopolymer gels for regenerative medicine. Biotechnol Lett 32:733–742

Kale S, Biermann S, Edwards C, Tarnowski C, Morris M, Long MW (2000) Three-dimensional cellular development is essential for ex vivo formation of human bone. Nat Biotechnol 18:954–958

Kim JK, Lee JS, Jung HJ, Cho JH, Heo JI, Chang YH (2007) Preparation and properties of collagen/modified hyaluronic acid hydrogel for biomedical application. J Nanosci Nanotechnol 7:3852–3856

Langbein L, Rogers MA, Winter H, Praetzel S, Beckhaus U, Rackwitz HR, Schweizer J (1999) The catalog of human hair keratins. I. Expression of the nine type I members in the hair follicle. J Biol Chem 274:19874–19884

Langbein L, Rogers MA, Winter H, Praetzel S, Schweizer J (2001) The catalog of human hair keratins. II. Expression of the six type II members in the hair follicle and the combined catalog of human type I and II keratins. J Biol Chem 276:35123–35132

Lee CH, Singla A, Lee Y (2001) Biomedical applications of collagen. Int J Pharm 221:1–22

Lynn AK, Yannas IV, Bonfield W (2004) Antigenicity and immunogenicity of collagen. J Biomed Mater Res B Appl Biomater 71B:343–354

Majno G, Gabbiani G, Hirschel BJ, Ryan GB, Statkov PR (1971) Contraction of granulation tissue in vitro: similarity to smooth muscle. Science 173:548–550

Makarem R, Humphries MJ (1991) LDV: a novel cell adhesion motif recognized by the integrin alpha 4 beta 1. Biochem Soc Trans 19:380S–382S

Mather ML, Tomlins PE (2010) Hydrogels in regenerative medicine: towards understanding structure-function relationships. Regen Med 5:809–821

Meena C, Mengi SA, Deshpande SG (1999) Biomedical and industrial applications of collagen. Proc Indian Acad Sci—Chem Sci 111:319–329

Nakaji-Hirabayashi T, Kato K, Iwata H (2008) Self-assembling chimeric protein for the construction of biodegradable hydrogels capable of interaction with integrins expressed on neural stem/progenitor cells. Biomacromolecules 9:1411–1416

Nerem RM (2000) Tissue engineering a blood vessel substitute: the role of biomechanics. Yonsei Med J 41:735–739

Ng KW, Khor HL, Hutmacher DW (2004) In vitro characterization of natural and synthetic dermal matrices cultured with human dermal fibroblasts. Biomaterials 25:2807–2818

Pathak A, Kumar S (2011) Biophysical regulation of tumor cell invasion: moving beyond matrix stiffness. Integr Biol 3:267–278

Reichl S (2009) Films based on human hair keratin as substrates for cell culture and tissue engineering. Biomaterials 30:6854–6866

Rouse JG, Van Dyke ME (2010) A review of keratin-based biomaterials for biomedical applications. Materials 3:999–1014

Schmedlen KH, Masters KS, West JL (2002) Photocrosslinkable polyvinyl alcohol hydrogels that can be modified with cell adhesion peptides for use in tissue engineering. Biomaterials 23:4325–4332

Sierpinski P, Garrett J, Ma J, Apel P, Klorig D, Smith T, Koman LA, Atala A, Van Dyke M (2008) The use of keratin biomaterials derived from human hair for the promotion of rapid regeneration of peripheral nerves. Biomaterials 29:118–128

Song E, Kim SY, Chun T, Byun HJ, Lee YM (2006) Collagen scaffolds derived from a marine source and their biocompatibility. Biomaterials 27:2951–2961

Spector M (2002) Novel cell-scaffold interactions encountered in tissue engineering: contractile behavior of musculoskeletal connective tissue cells. Tissue Eng 8:351–357

Szeverenyi I, Cassidy AJ, Chung CW, Lee BT, Common JEA, Ogg SC, Chen H, Sim SY, Goh WLR, Ng KW, Simpson JA, Chee LL, Eng GH, Li B, Lunny DP, Chuon D, Venkatesh A, Khoo KH, McLean WHI, Lim YP, Lane EB (2008) The human intermediate filament database: comprehensive information on a gene family involved in many human diseases. Hum Mutat 29:351–360

Thonhoff JR, Lou DI, Jordan PM, Zhao X, Wu P (2008) Compatibility of human fetal neural stem cells with hydrogel biomaterials in vitro. Brain Res 1187:42–51

Verma V, Verma P, Ray P, Ray AR (2008) Preparation of scaffolds from human hair proteins for tissue-engineering applications. Biomed Mater 3:12

Wrzesniewska-Tosik K, Adamiec J (2007) Biocomposites with a content of keratin from chicken feathers. Fibre Text East Eur 15:106–112

Yang CL, Hillas PJ, Baez JA, Nokelainen M, Balan J, Tang J, Spiro R, Polarek JW (2004) The application of recombinant human collagen in tissue engineering. Biodrugs 18:103–119